TOPOGRAPHIC CHARACTERIZATION OF COMPLEX LUNAR CRATERS WITH LOLA DATA. Jessica Kalynn[1], Catherine L. Johnson[1,2], Gordon R. Osinski[3], and Olivier Barnouin[4], [1]Department of Earth and Ocean Sciences, University of British Columbia, 6339 Stores Road, Vancouver, BC, V6T 1Z4, Canada, (jessicakalynn@hotmail.com; cjohnson@eos.ubc.ca), [2]Planetary Science Institute, 1700 East Fort Lowell, Suite 106, Tucson, AZ, 85719-2395 [3]Centre for Planetary Science and Exploration, University of Western Ontario, 1151 Richmond Street, London, Ontario, Canada, N6A 5B7; [4]The Johns Hopkins University Applied Physics Laboratory, 11100 John Hopkins Road, Laurel, MD 20723-6009.

Introduction: The morphometry of complex impact craters is important for understanding the cratering process and provides constraints on numerical models for crater formation [1]. Early investigations of lunar crater morphometry used shadow lengths in Earth-based imagery [2]. Using stereophotogrammetry derived from Apollo metric photos, and shadow lengths from Lunar Orbiter IV photos, Pike established depth (d) – diameter (D) relations for simple and complex craters [3]. Subsequent studies revisited this relationship, and investigated the relationship of central peak height (h_{cp}) and central peak diameter (D_{cp}) with crater diameter [4-7]. Typically these relationships are cast in the form $y = aD^b$ where y is d, h_{cp} or D_{cp}, and a and b are empirically determined parameters.

With the exception of one previous study of lunar basins and large complex craters [8], all of these analyses have been image-based due to the lack of absolute altimetric data of sufficient resolution to characterize crater topography. Lunar Orbiter Laser Altimeter (LOLA) data have an along-track spacing of ~26 m and a vertical accuracy of 0.1 m, permitting detailed investigations of the topography of lunar craters with diameters 10s km and smaller. In particular, the higher vertical precision and accuracy, and higher spatial resolution compared with *e.g.,* Clementine data are critical to the correct assessement of crater floor and rim elevations, and to be able to resolve the topography of central peaks.

In this study we examine the topography of fresh craters in the diameter range 15–110km. We assess how best to obtain a representative estimate of the elevation of crater rims, floors and (where observed) central peaks. We compare our results with previously published d-D and h_{cp}-D relationships [1,3-7] and ongoing complementary studies of craters in the transition regime between complex and multi-ring basins [9, 10].

Method: We use the lunar crater database of [11], and identify fresh craters, based on age and reported geological history [12,13]. We retain only Eratosthenian and Copernican age craters, and examine the literature and image data to check for subsequent modification (e.g. infilling by volcanics).

Our initial study uses LOLA gridded topography data for 45 craters with diameters between 15 and 110 km. The 64 pixel-per-degree LOLA grid was obtained from the PDS. Consequently, our measurements will have already been smoothed relative to measurements that can be made from individual LOLA tracks. Lambert equal area projections of the topography in and around each crater were made. We identify the radial extent of the central peak, crater floor and crater rim as a fraction of the published crater radius (image-based). Typically, the central peak falls within a circular region diameter, $D_{cp} = 0.2D$, the crater floor is within $0.55D$ and the rim crest lies in an annulus bounded by $0.95D$ and $1.1D$ (*e.g.,* Figure 1).

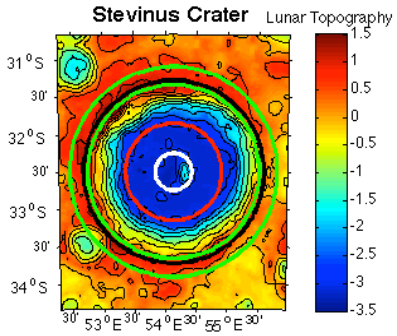

Figure 1. Topography (km) of Stevinus crater showing the central peak region (white circle), the floor region (red circle), and the rim (between green rings). Rings correspond to 0.2, 0.53, 0.95 and 1.1 times the crater diameter (black ring).

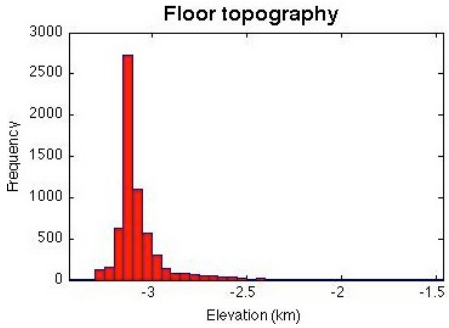

Figure 2. Elevation histogram for floor region of Stevinus crater. 50m bin intervals. The high elevation tail is attributed to the small number of elevations above -2.5 within the central peak region.

Given the agreement between the topographic crater rim position and previously defined crater diameters we use the published diameters and assume these to be error-free. For the floor and rim regions, we produce histograms of elevations, typically binned in 50m intervals (Figure 2), and examine the distributions and summary statistics such as the mean, mode, median, minimum and maximum. The mode of the distribution provides a good statistical representation of the crater floor elevation. In contrast, the minimum elevation may not be representative of most of the crater floor, as even the freshest floors are quite rough and can be further modified by subsequent craters. We take the characteristic floor elevation to be midway between the mode (h_{mode}) and minimum (h_{min}) and assign an uncertainty of (h_{mode}-h_{min})/2. The average uncertainty in floor elevations is ~120 m. The rim elevation was characterized similarly, taking the average of the mode and maximum elevation. The uncertainties in the rim elevations were about 600 m, reflecting rim height variability. The crater depth was taken as the difference in floor and rim elevations, with an error equal to the square root of the sum of the squared errors for the rim and the floor. The *d*-*D* relationship based on these 45 craters (Figure 3) is given by $d=0.68D^{0.44}$.

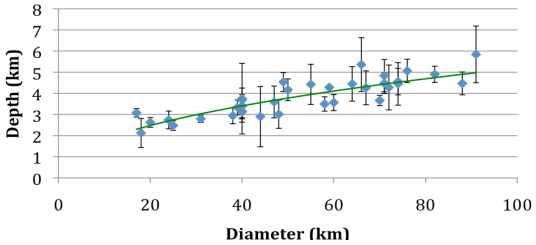

Figure 3. Depth-diameter relationship for 43 of the 45 craters in our initial study. Two craters with diameters in the range 100 to 110 km are excluded as they are shallow (depths < 5km) relative to the rest of the population.

The maximum height of the central peak was defined as the difference between the maximum elevation within the designated central peak region and the crater floor elevation. The uncertainty is given by the uncertainty in the floor elevation. The results are shown in Figure 4.

Discussion: The statistical characterization of crater floor and rim elevation can avoid bias introduced by local geology. For example, Leuschner crater (Figure 5) has an asymmetric rim topography. The maximum rim elevation, 5.45 km, is not representative of most of the rim (modal elevation of 3.93 km), leading to differences in crater depth estimates of up to 1.5 km.

Further studies will include additional craters in the diameter range specified here and will examine individual LOLA profile data. This is particularly important for proper characterization of central peaks that are small in spatial extent and may lie in between existing LOLA tracks. To better characterize individual craters, Lunar Orbiter and newer imaging data will be examined carefully to check for evidence for crater floor fill, rim weathering, pre-existing topography and subsequent cratering. Comparison of previous and new relationships will be made, as well as the influence of geological setting, in particular mare versus highland regions.

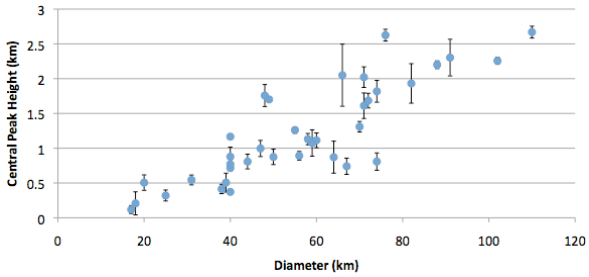

Figure 4. Relationship between central peak height and crater diameter for 45 lunar craters.

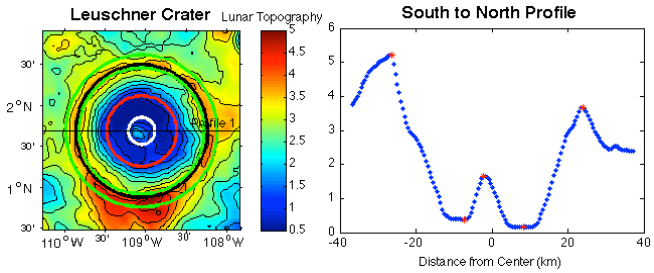

Figure 5. Topography (km) of Leuschner crater and a north-south profile. Note the elevation difference of ~1.5km between the south and north rims.

References: [1] Melosh H.J. (1983) *Impact Cratering: A Geologic Process.* Oxford Univ. Press, New York. [2] Baldwin R.B. (1963) *The Measure of the Moon*. Univ. Chicago Press, Chicago. [3] Pike R.A. (1974) *GRL, 1,* 291–293. [4] Pike R.A. (1977) *Proc. LSC 8th.,* 3427-3436 [5] Hale W. & Head J.W. (1979) *Proc. LPSC 10th,* 2623-2633; [6] Hale W. S. & Grieve R.A.F. (1982). *JGR, 87,* A65-A76. [7] Wood C.A. & Head J.W. (1976) *Proc. LSC. 7th,* 3629-3651 [8] Williams K.K. & Zuber M.T. (1997) *Icarus, 131*, 107–122 [9] Sori M.M. & Zuber M.T. (2010) *LPSC XXXXI,* #2202. [10] Baker et al. (2010), Fall AGU, P51C-1448. [11] Lossiak A. et al. (2009) *LPSC XXXX*, #1532. [12] Wilhelms D. E. (1987) *The Geologic History of the Moon,* US Government Printing Office, Washington, DC. [13] Hiesinger et al. (2010), *JGR,* 115 doi:10.1029/2009JE003380.